

## COMPARISON OF A SPECTRAL COLLOCATION METHOD AND SYMPLECTIC METHODS FOR HAMILTONIAN SYSTEMS

NAIRAT KANYAMEE AND ZHIMIN ZHANG

**Abstract.** We conduct a systematic comparison of a spectral collocation method with some symplectic methods in solving Hamiltonian dynamical systems. Our main emphasis is on non-linear problems. Numerical evidence has demonstrated that the proposed spectral collocation method preserves both energy and symplectic structure up to the machine error in each time (large) step, and therefore has a better long time behavior.

**Key Words.** Hamiltonian systems, spectral method, collocation, symplectic structure, energy conservation.

### 1. Introduction

Hamiltonian systems typically arise as models of conservative physical systems and have many applications in classical mechanics, molecular dynamics, hydrodynamics, electrodynamics, plasma physics, relativity, astronomy, and other scientific fields [29, 30]. They are an alternative and equivalent formalism of Newtonian and Lagrangian formalisms and become one of the most useful tools in the mathematical theory of physical and engineering sciences. Almost all real physical processes with negligible dissipation can be described in some way or another by Hamiltonian formalism [1].

The canonical system

$$(1) \quad \frac{dp_i}{dt} = -\frac{\partial H}{\partial q_i}, \quad \frac{dq_i}{dt} = \frac{\partial H}{\partial p_i}; \quad i = 1, 2, \dots, n$$

with given Hamiltonian function  $H(p_1, \dots, p_n; q_1, \dots, q_n)$  was first introduced by Hamilton in 1824. Since then, many famous scientists, such as Poincaré, Jacobi, Birkhoff, Weyl, Kolmogorov, and Arnold, studied the subject [1].

In addition to its elegance and symmetry, the Hamiltonian system has some remarkable properties, most important among which are its symplectic structure and optimality for energy preservation. Any good numerical scheme should be able to replicate as many of these physical properties as possible. The symplectic structure is in nature volume-preserving. Traditional ODE solvers such as Runge-Kutta, multi-step methods usually do not preserve the symplectic structure and energy, and as a consequence, numerical trajectories tend to gradually drift away from the true solution trajectories in a phenomenon called phase shift. The idea of developing numerical methods that maintain the symplectic structure was first studied in a general setting by Feng in the 1980' [10]. This was followed by a successful systematic study of designing so-called symplectic algorithms [11, 12,

---

Received by the editors June 1, 2009 and, in revised form, March 22, 2010.

2000 *Mathematics Subject Classification.* 65N20, 49J40.

This research was supported in part by the National Science Foundation under grant DMS-0612908.

13, 14, 15, 16, 17, 26, 33]. But, none of these symplectic algorithms is energy-preserving in general. Indeed, it was proved that there exists no energy preserving symplectic algorithm for general non-linear Hamiltonian systems [19, 9]. On the other hand, Galerkin type methods such as finite element methods are well-known to preserve energy. Now we face a dilemma and have to choose between preserving energy and preserving symplectic structure. Some argue that for highly oscillatory problems, preserving energy may be more important than the symplectic structure [7, 8, 32, 4, 18].

In this paper, we introduce an algorithm based on spectral collocation to preserve both energy and volume (symplectic structure) up to numerically negligible error terms. If the error term is so small that it reaches the machine epsilon – the computer round-off error, then the algorithm is practically energy and volume preserving. We shall use a series numerical benchmark problems to demonstrate that our methods are effective and much accurate than symplectic methods with the similar computational cost.

There have been some recent attempts in using spectral method [35] and spectral collocation method [22] to solve ODEs. In this work, we carry on a systematic comparison between the proposed spectral collocation method and symplectic methods. For more references regarding spectral and spectral collocation methods, the reader is referred to [2, 3, 5, 6, 20, 21, 27, 31, 34, 37] and references therein.

## 2. The algorithm

To simplify the discussion, we use the case  $n = 1$  in (1) to illustrate the idea. Consider the nonlinear Hamiltonian system

$$p' = -\frac{\partial H}{\partial q} = f(p, q), \quad q' = \frac{\partial H}{\partial p} = g(p, q), \quad p(0) = p_0, \quad q(0) = q_0,$$

where  $f$  and  $g$  are nonlinear functions. We use either the Chebyshev-Gauss-Lobatto or the Legendre-Gauss-Lobatto collocation methods to solve it. We solve the system on  $[0, r]$  first, then use the obtained values  $(p(r), q(r))$  as an initial condition to repeat the process on  $[r, 2r]$ , and so on .... Here  $r$  could be large, a convenient choice is  $r = 2$ .

Let  $t_0 < t_1 < \dots < t_N$  be collocation points where  $t_0 = 0$  and  $t_N = r$ . We interpolate  $p$  and  $q$  as

$$p_N(t) = \sum_{j=0}^N p(t_j) \ell_j(t), \quad q_N(t) = \sum_{j=0}^N q(t_j) \ell_j(t),$$

where  $\ell_j$  is the Lagrange nodal basis function satisfying  $\ell_j(t_i) = \delta_{ij}$ .

We are seeking numerical approximations of  $(p(t_j), q(t_j))$ , denoted as  $(p_j, q_j)$ . In the literature of the spectral method, the explicit form of the differentiation matrix  $D = (d_{ij})_{i,j=0}^N$  is known [2, 3, 5, 6, 21, 34] with  $d_{ij} = \ell_j'(t_i)$ . Note that the rank of the  $(N+1) \times (N+1)$  matrix  $D$  is  $N$ . Therefore, we may solve the system

$$\begin{aligned} d_{11}p_1 + d_{12}p_2 + \dots + d_{1N}p_N &= f(p_1, q_1) - d_{10}p_0 \\ &\vdots \\ d_{N1}p_1 + d_{N2}p_2 + \dots + d_{NN}p_N &= f(p_N, q_N) - d_{N0}p_0 \\ d_{11}q_1 + d_{12}q_2 + \dots + d_{1N}q_N &= g(p_1, q_1) - d_{10}q_0 \\ &\vdots \\ d_{N1}q_1 + d_{N2}q_2 + \dots + d_{NN}q_N &= g(p_N, q_N) - d_{N0}q_0 \end{aligned}$$

to obtain  $\mathbf{p} = (p_1, p_2, \dots, p_N)^T$  and  $\mathbf{q} = (q_1, q_2, \dots, q_N)^T$ , and use the rest two equations

$$\begin{aligned} d_{01}p_1 + d_{02}p_2 + \dots + d_{0N}p_N &= g(p_0, q_0) - d_{00}p_0, \\ d_{01}q_1 + d_{02}q_2 + \dots + d_{0N}q_N &= g(p_0, q_0) - d_{00}q_0 \end{aligned}$$

to estimate the error.

If we denote

$$\mathbf{f}(\mathbf{p}, \mathbf{q}) = \begin{pmatrix} f(p_1, q_1) - d_{10}p_0 \\ f(p_2, q_2) - d_{20}p_0 \\ \vdots \\ f(p_N, q_N) - d_{N0}p_0 \end{pmatrix}, \quad \mathbf{g}(\mathbf{p}, \mathbf{q}) = \begin{pmatrix} g(p_1, q_1) - d_{10}q_0 \\ g(p_2, q_2) - d_{20}q_0 \\ \vdots \\ g(p_N, q_N) - d_{N0}q_0 \end{pmatrix}$$

Then we design a numerical iteration in the matrix form

$$\begin{pmatrix} \tilde{D} & 0 \\ 0 & \tilde{D} \end{pmatrix} \begin{pmatrix} \mathbf{p}^{new} \\ \mathbf{q}^{new} \end{pmatrix} = \begin{pmatrix} \mathbf{f}(\mathbf{p}^{old}, \mathbf{q}^{old}) \\ \mathbf{g}(\mathbf{p}^{old}, \mathbf{q}^{old}) \end{pmatrix},$$

where  $\tilde{D}$  is a  $N \times N$  matrix by eliminating the first row and the first column of  $D$ . This format is valid for any  $n$  in (1). In the process, we may use Gauss-Seidal type iteration to update the information as soon as possible.

### 3. Conservation properties

Theoretical study shows that the solution of a Hamiltonian system can be described by an evolution semigroup which is a symplectic mapping for any fixed  $t$ . Furthermore, the Hamiltonian is conserved along trajectories.

$$H(p_N(t_N), q_N(t_N)) = H(p_N(t_0), q_N(t_0)) = H(p_0, q_0),$$

i.e., the collocation method preserves the energy up to numerical integration error. In many practical problems, due to the analytic nature of  $H(p, q)$  and spectral accuracy, we are able to control the numerical quadrature error to the machine epsilon, i.e.,  $10^{-15}$  with a reasonable  $N$ , say,  $N \leq 20$ . In this case, the spectral collocation we introduced preserves the energy in practice.

Another important feature or property of the Hamiltonian system is the symplectic structure, namely, the Jacobi matrix of the transformation

$$\begin{pmatrix} \frac{\partial \mathbf{z}_N}{\partial \mathbf{z}_0} \end{pmatrix}, \quad \mathbf{z} = \begin{pmatrix} \mathbf{p} \\ \mathbf{q} \end{pmatrix}$$

satisfies

$$\begin{pmatrix} \frac{\partial \mathbf{z}_N}{\partial \mathbf{z}_0} \end{pmatrix} J \begin{pmatrix} \frac{\partial \mathbf{z}_N}{\partial \mathbf{z}_0} \end{pmatrix}^T = J, \quad J = \begin{pmatrix} 0 & I_N \\ -I_N & 0 \end{pmatrix}.$$

Note that with the above notation, the Hamiltonian system can be written as

$$\mathbf{z}_t = J^{-1} H_{\mathbf{z}}.$$

Based on the high accuracy of the spectral Galerkin and spectral collocation methods, it is reasonable to expect that

$$\begin{pmatrix} \frac{\partial \mathbf{z}_N}{\partial \mathbf{z}_0} \end{pmatrix} J \begin{pmatrix} \frac{\partial \mathbf{z}_N}{\partial \mathbf{z}_0} \end{pmatrix}^T = J + O(e^{-\sigma N}).$$

This has a significant meaning in practice. When the error reaches the machine epsilon somewhere around  $10^{-15}$ , the scheme is in practice volume preserving (i.e., preserves the symplectic structure)! The reader is referred to [36] for more conservation properties of numerical methods.

#### 4. Numerical tests

In this numerical study, we are interested in long-time behavior of the Hamiltonian system, which many science and engineering problems need to predict, see, e.g., [23, 24, 25, 18]. Traditional finite difference, finite element, and Runge-Kutta methods fail when time runs sufficiently large, even those symplectic structure preserving algorithms. Our numerical tests on Hamiltonian systems demonstrate that the spectral collocation methods preserve both energy and volume very well even at for large  $t$ . The numerical solution follows the trajectory nicely without a phase shift.

In coding, we install  $\tilde{D}^{-1}$  since it will be used repeatedly - in some cases, billions of times. It is well known that the condition number of  $\tilde{D}$  is  $O(N^2)$ . For relatively large values of  $N$ , it would be ideal to develop an explicit formula for  $\tilde{D}^{-1}$  instead of inverting the explicit form of  $\tilde{D}$ .

For the numerical examples below, we use  $r = 1$  for the spectral collocation. The reasonable values for  $r$  is within the interval  $[0.75, 2]$ . In each updating process, we compare the maximum pointwise errors,

$$\max_{1 \leq j \leq N} (\|\mathbf{p}^{new} - \mathbf{p}^{old}\|(t_j)\|_{L^\infty}, \|\mathbf{q}^{new} - \mathbf{q}^{old}\|(t_j)\|_{L^\infty})$$

and set the tolerance as  $10^{-15}$  together with maximum iteration numbers, 1000, to terminate the iterative process. The initial guesses to start the spectral collocation are  $N \times 1$  vectors  $(p_0, \dots, p_0)^T$  and  $(q_0, \dots, q_0)^T$  where  $p_0, q_0$  are the initial values.

We compare numerical results from the spectral collocation method with the results from symplectic methods provided in the Appendix by using the maximum pointwise norm,  $\|(\mathbf{p} - \mathbf{p}_N)(t_j)\|_{L^\infty}$  on the terminal interval. Symplectic schemes 1,2,3 and 4 are second order schemes where scheme 1 is a second order midpoint Euler scheme and Scheme 3 and 4 are specially designed for the threefold symmetry and Henon-Heiles systems, respectively. The CPU times (after the graphic outputs) of both methods is considered by using Lenovo X61, Core 2 Duo 1.8GHz, RAM 3GB.

**Example 1:** Consider a linear system of ordinary differential equations

$$\begin{aligned} p'(t) &= -4q(t) \\ q'(t) &= p(t) \end{aligned}$$

with initial condition  $p(0) = 0$ ,  $q(0) = 0.6$ .

The Hamiltonian for this system is given by  $H(p, q) = \frac{1}{2}p^2 + 2q^2$ . The exact solutions are  $p(t) = -1.2 \sin(2t)$  and  $q(t) = 0.6 \cos(2t)$ . The initial energy  $H(p_0, q_0) = H_0 = 0.72$ .

We compare the spectral collocation with Symplectic 1 and Symplectic 2. Figure 1 represents the end behavior of each method. From the graphs, we can barely see the difference between the exact and numerical solutions from the spectral collocation ( $t = 10^6$ ) while the phase shift is visible for the symplectic methods at  $t = 2000$ .

Tables 1 and 2 provide the maximum errors on the end interval of energy  $H$ ,  $p(t)$ ,  $q(t)$ , and the CPU times used. The spectral collocation method provides more nodal data with similar CPU times, or can go further in term of time  $t$  than a simple symplectic method as shown in Table 1. This means that the spectral collocation method is less expensive in a long run compared with a simple symplectic method.

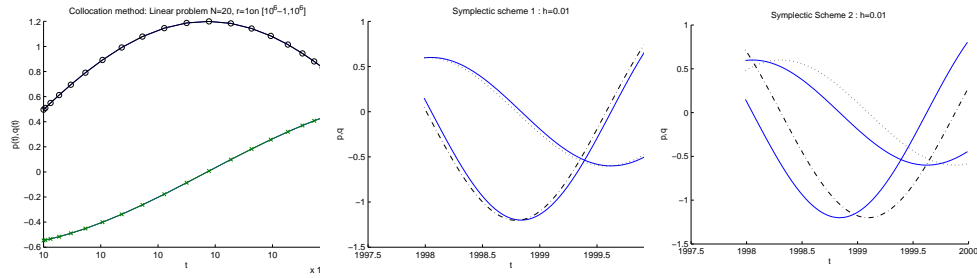


FIGURE 1. Graph of solution  $p, q$  versus  $t$  by (a) spectral collocation when  $N = 20$  on  $[10^6 - 1, 10^6]$  (p:-o-,q:-x-); (b) Symplectic 1,  $h=0.01$  on  $[1998,2000]$  (p:dash,q:dot); (c) Symplectic 2,  $h=0.01$  on  $[1998,2000]$

Table 2 shows the CPU times used when the end point is fixed as  $t = 100$ . With a low number of collocation points  $N$  and small step size  $h$  (symplectic), the errors are almost the same from both methods but the CPU times used for the symplectic method is much longer than the spectral method.

	time(secs)	Error in Energy	Error in $p(t)$	Error in $q(t)$
Colloc. $N=20, [0, 10^9]$	621	$2.294946 \times 10^{-10}$	$2.228963 \times 10^{-10}$	$9.142997 \times 10^{-10}$
Symp 1, $h=0.01, [0, 2000]$	484	$2.884887 \times 10^{-3}$	$7.999879 \times 10^{-2}$	$6.323009 \times 10^{-1}$
Symp 1, $h=0.01, [0, 2350]$	642	$3.391444 \times 10^{-3}$	$9.409463 \times 10^{-2}$	$4.703431 \times 10^{-2}$
Symp 1, $h=0.01, [0, 10^9]$	> 6hrs			
Symp 2, $h=0.01, [0, 2000]$	445	$7.200007 \times 10^{-7}$	$4.001598 \times 10^{-2}$	$3.160331 \times 10^{-1}$
Symp 2, $h=0.01, [0, 2250]$	603	$7.200007 \times 10^{-7}$	$7.090428 \times 10^{-1}$	$3.543846 \times 10^{-1}$
Symp 2, $h=0.01, [0, 10^9]$	> 5hrs			

TABLE 1. Comparison of CPU times between the three methods.

	time(secs)	Error in Energy	Error in $p(t)$	Error in $q(t)$
Colloc., $N=10, [0, 100]$	1.06	$6.185242 \times 10^{-6}$	$5.631718 \times 10^{-6}$	$2.787909 \times 10^{-6}$
Symp 1, $h=0.001, [0, 100]$	78.29	$7.188678 \times 10^{-7}$	$3.958494 \times 10^{-5}$	$1.994939 \times 10^{-5}$
Symp 1, $h=0.0008, [0, 100]$	191.98	$4.600998 \times 10^{-7}$	$2.533450 \times 10^{-5}$	$1.276760 \times 10^{-5}$
Symp 1, $h=0.0001, [0, 100]$	591.45	$1.796755 \times 10^{-7}$	$9.896375 \times 10^{-6}$	$4.987343 \times 10^{-6}$

TABLE 2. Comparison of CPU times between the two methods with the same order of errors.

Figure 2 shows the rate of convergence of the numerical error for  $p$  from both methods. The spectral collocation gives a super-exponential rate [40, 41]. The convergence rate is of order  $(\frac{1}{N})^{(0.75N)}$  for the spectral collocation and  $h^2$  for the symplectic scheme 1 (second order scheme).

The rest examples are nonlinear Hamiltonian systems.

**Example 2:** Consider a system with a Hamiltonian  $H(p, q) = p^2 - q^2 + q^4$  [12].

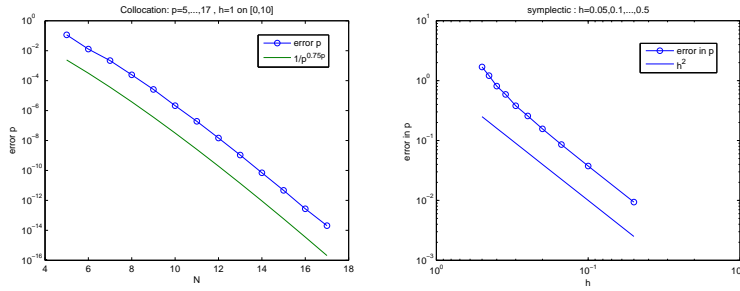


FIGURE 2. (a) Collocation method,  $N=5,6,\dots,17$  on  $[0,10]$ ; (b) Symplectic 1,  $h=0.05,0.1,\dots,0.5$  on  $[0,10]$

The corresponding system of nonlinear ODEs is

$$\begin{aligned} p'(t) &= -\frac{\partial H}{\partial q} = 2q - 4q^3 \\ q'(t) &= \frac{\partial H}{\partial p} = 2p \end{aligned}$$

with initial condition  $p(0) = p_0, q(0) = q_0$ .

There are three equilibrium points for this system:  $E_1 = (\bar{p}, \bar{q}) = \mathbf{0}, E_2 = (0, \frac{1}{\sqrt{2}})$  and  $E_3 = (0, -\frac{1}{\sqrt{2}})$ . The zero equilibrium point is a saddle point and the other two are centers. As a result, we have to be careful when we choose initial values for our system in order to avoid the neighborhood of  $(0, 0)$ . The iterative method will not converge otherwise.

For the spectral collocation, the range of the initial condition for  $q$  that can be used in order for the numerical solution to converge is about 0.625 to 0.88. For the oscillatory behavior, we choose  $q_0$  within 0.625-0.7 and 0.715-0.88. If we choose a number close to the equilibrium  $(0, 0.7071067811865475)$ , we will get almost a straight line. The initial values were chosen as  $p_0 = 0, q_0 = 0.73$ . This gives  $H(p_0, q_0) = H_0 = -0.24891758$ .

Figure 3 represents phase plots of  $p$  and  $q$ . We can see that with Symplectic 1, the loop is thicker (there is a phase shift) and with the spectral collocation method, the loop is thinner and sharper.

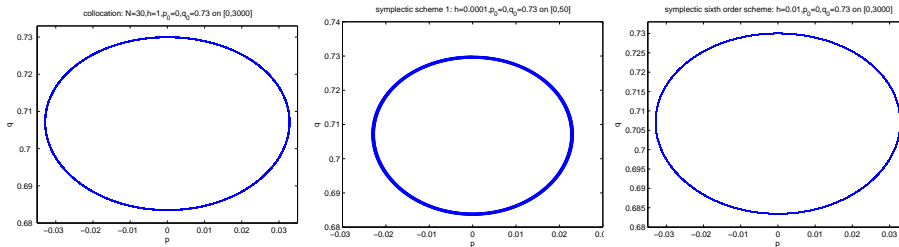


FIGURE 3. Phase plot  $q$  versus  $p$  by (a) spectral collocation when  $N = 30$  on  $[0, 3000]$ ; (b) Symplectic 1  $h=0.0001$  on  $[0,50]$ ; (c) symplectic sixth order  $h=0.01$  on  $[0,3000]$ .

The CPU times for each method is shown in Table 3. We use  $h = 0.001$  for the symplectic schemes 1, 2 and  $h = 0.01$  for a sixth order symplectic method [39]. Similar to the linear case, the spectral collocation is more effective in a long run. It takes less CPU times than all three symplectic methods.

	time(secs)	Error in Energy
Collocation, N=50 on [0,10000]	2898	$5.2735593669 \times 10^{-15}$
Collocation, N=30 on [0,5000]	668	$7.6605388699 \times 10^{-15}$
Symplectic 1 on [0,450]	2849	$9.9279222845 \times 10^{-4}$
Symplectic 1 on [0,500]	3585	$1.0088809618 \times 10^{-3}$
Symplectic 1 on [0,1000]	> 2 hrs	
Symplectic 2 on [0,460]	3010	$3.8086767073 \times 10^{-10}$
Symplectic 2 on [0,1000]	> 2 hrs	
Symplectic 6th order on [0,4200]	2602	$5.4956039718 \times 10^{-15}$
Symplectic 6th order on [0,5000]	9833	$7.6327832942 \times 10^{-15}$
Symplectic 6th order on [0,10000]	>3hrs	

TABLE 3. Comparison of CPU times between the four methods.

Table 4 compares the CPU times used on the same interval [0,1000] for the sixth order symplectic method and the spectral collocation method. We can see that both methods give the same order of error in energy but the symplectic method takes much longer time.

	time(secs)	Error in Energy
Collocation, N=18 on [0,1000]	36	$5.7176485768 \times 10^{-15}$
Symplectic 6th order h=0.015 on [0,1000]	12.61	$3.6359804056 \times 10^{-14}$
Symplectic 6th order h=0.01 on [0,1000]	80	$4.7739590058 \times 10^{-15}$

TABLE 4. Comparison of CPU times between the spectral collocation and the sixth order symplectic method with the same order of errors.

The convergence rates of the energy  $H$  for both methods are shown in Figure 4. The rate is  $(\frac{1}{N})^{(0.6N)}$  for the spectral collocation,  $O(h^2)$  for the symplectic scheme 2, and  $O(h^6)$  for the sixth order symplectic scheme.

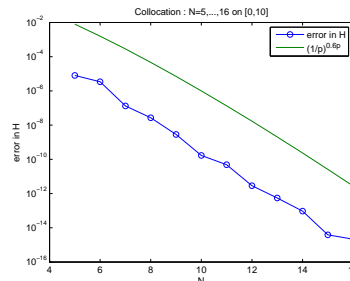


FIGURE 4. Error in  $H$  and  $(\frac{1}{N})^{(0.6N)}$  versus  $N = 5, 6, \dots, 16$  by spectral collocation on [0, 10].

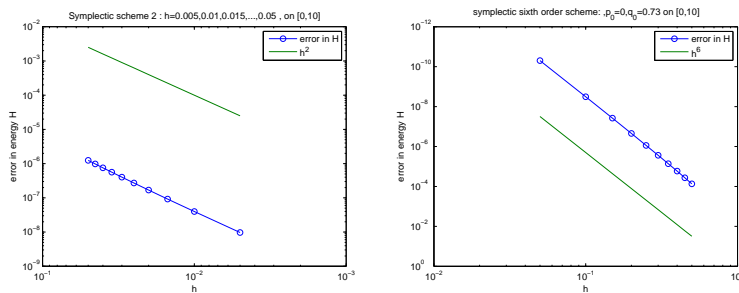


FIGURE 5. (a) Error in  $H$  by Symplectic 2 with  $h=0.005,0.01,0.015,\dots,0.05$ , on  $[0,10]$ ; (b) Error in  $H$  by the sixth order symplectic scheme.

**Example 3:** Threefold symmetry Hamiltonian system [13].

Consider a  $k$ -fold rotational symmetry system in phase plane with Hamiltonian

$$H_k(p, q) = \sum_{j=1}^k \cos(p \cos(\frac{2\pi j}{k}) + q \sin(\frac{2\pi j}{k})).$$

For  $k = 3$ , the three axis-symmetric Hamiltonian system is,

$$H(p, q) = \cos(p) + \cos(-\frac{1}{2}p + \frac{\sqrt{3}}{2}q) + \cos(\frac{1}{2}p + \frac{\sqrt{3}}{2}q).$$

The corresponding system of nonlinear ODE for this  $H$  is

$$\begin{aligned} p'(t) &= -\frac{\partial H}{\partial q} = \frac{\sqrt{3}}{2} \sin(-\frac{1}{2}p + \frac{\sqrt{3}}{2}q) + \frac{\sqrt{3}}{2} \sin(\frac{1}{2}p + \frac{\sqrt{3}}{2}q) \\ q'(t) &= \frac{\partial H}{\partial p} = -\sin(p) + \frac{1}{2} \sin(-\frac{1}{2}p + \frac{\sqrt{3}}{2}q) - \frac{1}{2} \sin(\frac{1}{2}p + \frac{\sqrt{3}}{2}q) \end{aligned}$$

with initial condition  $p(0) = \pi$ ,  $q(0) = 0$ . In this case,  $H_0 = -1$ .

Figure 6 contains the graphs of  $p, q$  with respect to time  $t$ . The result from the symplectic method does not make a right corner like the one from the spectral collocation method. We can see it clearly if we consider the phase plot of the results. The phase plot from a symplectic method has fuzzy corners compared with sharp-corner hexagon from the spectral collocation as shown in Figure 7. Note that the possible solutions for threefold symmetry Hamiltonian system contain equilateral triangles and hexagons depending on the initial conditions. We consider only a hexagon case in this example. For the symplectic method, the smaller the  $h$ , the more horizontally stretched the graph is. The graph tends to have the same behavior as the collocation method when the size of  $h$  decreases.

Table 5 shows convergent rates for the energy  $H$  and the CPU times. We use  $h = 0.001$  for the symplectic schemes 3. The spectral collocation method used 45 minutes to obtain data in  $[0, 10000]$  but with the same time used, the symplectic method produces data approximately on  $[0, 450]$  with much lower accuracy.

The convergence rates for both methods are shown in Figure 8. For the spectral collocation method, the error drops down to machine error with relatively small  $N$ .

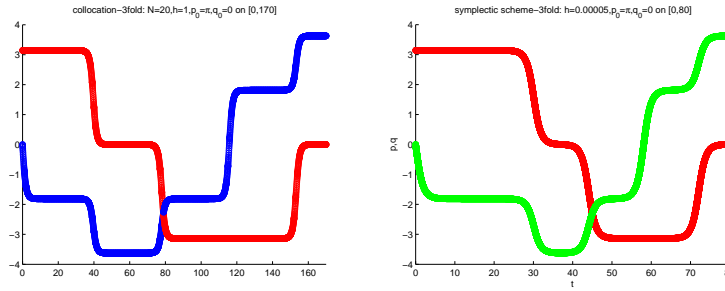


FIGURE 6. Graph of  $p$  (upper) and  $q$  (lower) versus  $t$  (a) by Collocation method when  $N = 20$  on  $[0, 170]$ ; (b) by Symplectic 3  $h = 0.00005$  on  $[0, 80]$ .

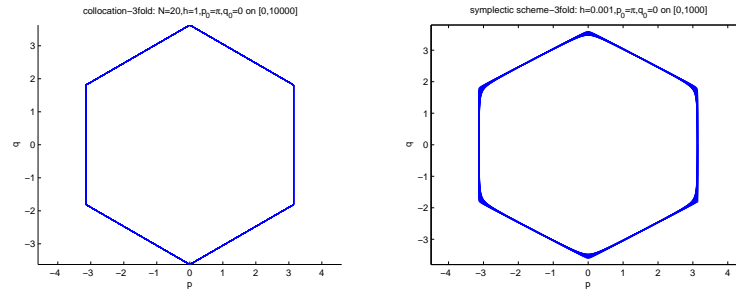


FIGURE 7. Phase plot  $q$  versus  $p$  (a) by spectral collocation when  $N = 20$  on  $[0, 10000]$ ; (b) by Symplectic 3 when  $h=0.001$  on  $[0, 1000]$

	time(secs)	Error in Energy
Collocation, $N=20$ on $[0, 1000]$	33	$2.5368596112 \times 10^{-13}$
Collocation, $N=20$ on $[0, 10000]$	2725(45mins)	$2.7539082125 \times 10^{-12}$
Symplectic 3 on $[0, 400]$	2190	$6.425967063916294 \times 10^{-3}$
Symplectic 3 on $[0, 600]$	5360(89mins)	$1.0537382086 \times 10^{-2}$

TABLE 5. Comparison of CPU times between the two methods.

**Example 4:** The Henon-Heiles(HH) system [14, 15].

The Henon-Heiles(HH) Hamiltonian was introduced in the study of galactic dynamics to describe the motion of stars around the galactic center.

$$H(p_1, p_2, q_1, q_2) = \frac{1}{2}(p_1^2 + p_2^2 + q_1^2 + q_2^2) + q_1^2 q_2 - \frac{1}{3} q_2^3.$$

The terms  $q_1^2, q_2^2$ , form a potential well, which is responsible for the oscillations of the particle (the first four terms are related to the Kinetic energy). The last two terms,  $q_1^2 q_2, \frac{1}{3} q_2^3$  are responsible for the existence of the exits from the orbit.

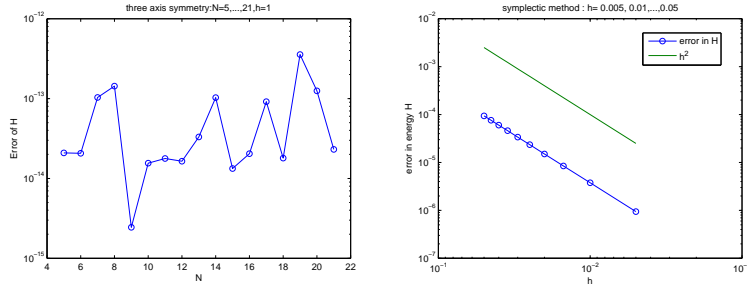


FIGURE 8. (a) Error in  $H$  versus  $N$  when  $N = 5, 6, \dots, 21$  by spectral collocation on  $[0, 500]$ ; (b) Error in  $H$  versus  $h$  when  $h = 0.005, 0.01, \dots, 0.05$  by the symplectic scheme 3 on  $[0, 10]$

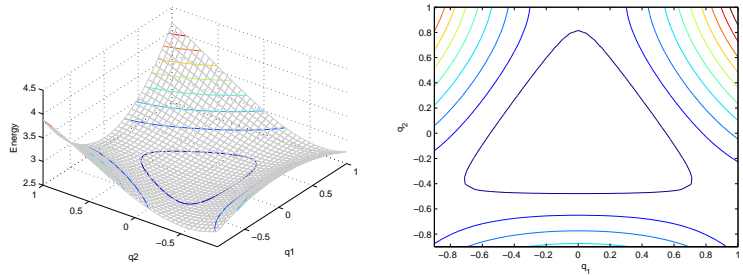


FIGURE 9. Graph of contour plot of energy  $H$  when  $q_2$  and  $q_1$  vary and  $p_1 = 2, p_2 = 1$  are fixed (a) 3-D (b) 2-D

There are four equilibrium points for this system which are  $E_1 = (\bar{p}_1, \bar{p}_2, \bar{q}_1, \bar{q}_1) = \mathbf{0}$ , a center,  $E_2 = (0, 0, 0, 1)$ ,  $E_3 = (0, 0, \frac{\sqrt{3}}{2}, -\frac{1}{\sqrt{2}})$  and  $E_4 = (0, 0, -\frac{\sqrt{3}}{2}, -\frac{1}{\sqrt{2}})$ , saddle points. As a result, there are three exits for the energy to escape according to the three saddle points. The total energy  $H_E = 0$  for  $E_1$  and  $H_E = \frac{1}{6}$  for  $E_2, E_3$ , and  $E_4$ . If the initial energy is far beyond this  $H_E$ , the particles wander inside the region for a certain time in the scattering region until they cross one of the three energy line and escape to infinity. In other words, when the initial  $H < \frac{1}{6}$ , the solution is regular; when  $H > \frac{1}{6}$ , the solution is chaotic. Note that the time they spent in bounded region is named “escape time”. The higher the energy, the shorter escape times are found.

Figure 9 shows the phase plots for potential energy  $H$  when  $p_1 = 2, p_2 = 1$  are fixed,  $q_2$  and  $q_1$  vary. We can see that the three exits for the energy are at the three saddle points  $E_2, E_3, E_4$  located at three corners of an equilateral triangle.

The system of nonlinear ODE for this  $H$  is

$$\begin{aligned} p_1'(t) &= -\frac{\partial H}{\partial q_1} = -q_1 - 2q_1 q_2 \\ p_2'(t) &= -\frac{\partial H}{\partial q_2} = -q_2 - q_1^2 + q_2^2 \\ q_1'(t) &= \frac{\partial H}{\partial p_1} = p_1 \\ q_2'(t) &= \frac{\partial H}{\partial p_2} = p_2 \end{aligned}$$

We select two different sets of initial conditions. The first set represents a regular case with

$$p_1(0) = 0.011, p_2(0) = 0, q_1(0) = 0.013, q_2(0) = -0.4; \quad H_0 = 0.101410733 < 1/6.$$

The second set is a chaotic case with

$$p_1(0) = \sqrt{2 \times 0.15925}, p_2(0) = q_1(0) = q_2(0) = 0.12; \quad H_0 = 0.18200200 > 1/6.$$

Figure 10 shows the chaotic solution and the phase plot when the particle wanders in the bounded region until it crosses the energy threshold line and escapes. Figure 11 represents phase plots of a regular solution from both methods. The trajectory from symplectic method is denser than the one from collocation method.

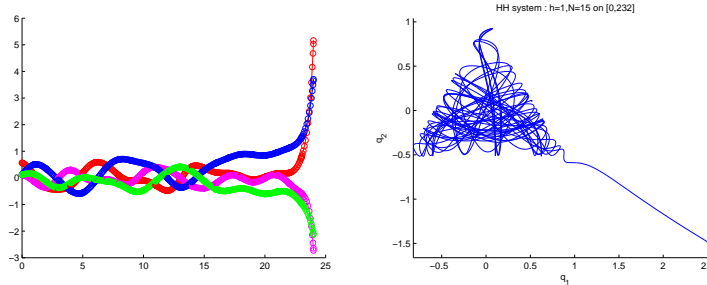


FIGURE 10. Chaotic solution by spectral collocation  $N = 15$  (a) on  $[0, 24]$ ; (b) phase plot  $q_2$  versus  $q_1$  on  $[0, 232]$ .

The error in energy,  $H$ , and the CPU times are presented in the table. We choose initial conditions from the regular case. We use  $h = 0.001$  for Symplectic scheme 4.

	time(secs)	Error in Energy
Collocation, N=20 on $[0, 10000]$	2691	$1.9004658957 \times 10^{-12}$
Collocation, N=20 on $[0, 1000]$	25	$1.9076407120 \times 10^{-13}$
Symplectic 4 on $[0, 65]$	21	$6.0026862363 \times 10^{-9}$
Symplectic 4 on $[0, 200]$	970(16mins)	$6.0026862363 \times 10^{-5}$
Symplectic 4 on $[0, 1000]$	>2hrs	

TABLE 6. Comparison of CPU times between the two methods.

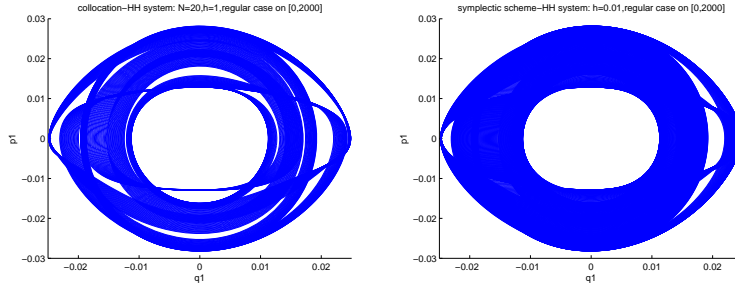


FIGURE 11. Phase plot of a regular case on  $[0,2000]$  (a) by the spectral collocation  $N = 20$ ; (b) by Symplectic 4  $h=0.01$ .

The rate of convergence in energy using the regular initial values is shown in Figure 12. Spectral collocation gives the rate in the order of  $(\frac{1}{N})^{(0.85N)}$  and the symplectic scheme 4 is of order one.

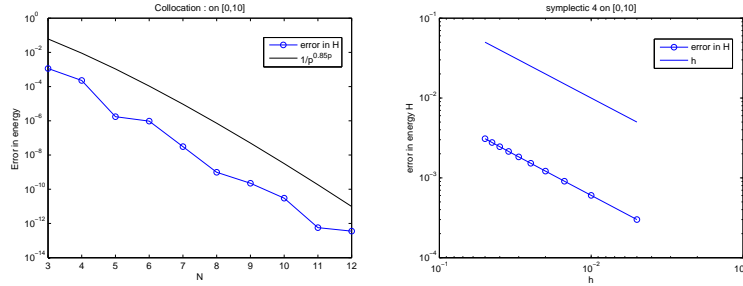


FIGURE 12. (a) Error in  $H$  and  $(\frac{1}{N})^{(0.85N)}$  versus  $N$  when  $N = 3, 4, \dots, 12$  by spectral collocation on  $[0, 10]$ ; (b) Error in  $H$  versus  $h$  when  $h = 0.005, 0.01, \dots, 0.05$  by Symplectic 4 on  $[0, 10]$ .

**Example 5:** A modified Two-body Problem [38].

The Hamiltonian for this system is  $H = T + V$  where  $T = \frac{1}{2}\|\mathbf{p}\|^2$  and  $V = -\frac{1}{\|\mathbf{q}\|} - \frac{\epsilon}{2\|\mathbf{q}\|^3}$ . Thus

$$H(\mathbf{p}, \mathbf{q}) = \frac{1}{2}\|\mathbf{p}\|^2 - \frac{1}{\|\mathbf{q}\|} - \frac{\epsilon}{2\|\mathbf{q}\|^3}.$$

where  $\epsilon$  is a small perturbation parameter.

The system of nonlinear ODEs for this energy is

$$\begin{aligned} p_1'(t) &= -\frac{q_1}{\sqrt{(q_1^2 + q_2^2)^3}} - \frac{3\epsilon q_1}{2\sqrt{(q_1^2 + q_2^2)^5}} \\ p_2'(t) &= -\frac{q_2}{\sqrt{(q_1^2 + q_2^2)^3}} - \frac{3\epsilon q_2}{2\sqrt{(q_1^2 + q_2^2)^5}} \\ q_1'(t) &= p_1 \\ q_2'(t) &= p_2 \end{aligned}$$

with initial conditions  $p_1(0) = p_{10}, p_2(0) = p_{20}, q_1(0) = q_{10}, q_2(0) = q_{20}$ .

This is a modification of the two-body problem. It is about the system of two massive bodies that attract each other by the gravitational force. We are seeking for the positions and velocities of those two bodies. The first body is located at the origin. The second body is located where its coordinates are  $(q_1, q_2)$  and the corresponding velocity is  $(q_1', q_2') = (p_1, p_2)$ . This model describes the motion of a particle in a plane. A particle in this model is attracted gravitationally by a slightly oblate sphere instead of a point mass. The attracting body rotates symmetrically with respect to an axis perpendicular to the plane of the particle. If there is no perturbation ( $\epsilon$ ), the problem is just a regular two-body problem[15].

Besides the energy  $H$ , this system also preserves the angular momentum which is  $p^T B q$ , where  $B = J$  for this problem, i.e  $\frac{d(p^T J q)}{dt} = 0 \Rightarrow p^T J q = p_0^T J q_0$ . We use the initial values  $p_1(0) = 0, p_2(0) = \sqrt{\frac{1+e}{1-e}}, q_1(0) = 1-e, q_2(0) = 0$ , where  $e$  is the eccentricity of the orbit. Here if we choose  $e$  closer to one, the solution tends to diverge and does not conserve energy well for both spectral collocation and symplectic methods. We choose  $e$  small enough in order for the solution to converge to an equilibrium point.

We compare the spectral collocation with a second order symplectic method. The eccentricity  $e$  is 0.001 (almost a circle) for the numerical test. Both methods preserve the structure. Figures 13 represents phase plots by spectral collocation with a perturbation value  $\epsilon = 0.005$ . For all reasonable  $N$  and  $h$ , the solutions from both methods are almost the same with a slightly thicker orbit at the left and right corners for symplectic method (not shown). Note that with a larger perturbation, the body rotates in an oblique pattern. If we compare the time and error, the spectral method gives a better result.

Table 7 represents the error in energy  $H$ , error in the angular momentum, and the CPU times. For these initial conditions, both errors and CPU times from the spectral collocation are better than a symplectic method. However, if we change the initial conditions to  $p_{10} = 0.1, p_{20} = 0.9, q_{10} = q_{20} = 1$ , the errors from both methods are almost in the same order but the spectral collocation is time efficient as we can see from Table 8 with the two-body case ( $\epsilon = 0$ ).

The convergence rates for both methods are shown in Figure 14. The convergence rate for symplectic scheme is of order three and  $(\frac{1}{N})^{(1.1N)}$  for spectral collocation.

**Example 6:** The Three-body system [28].

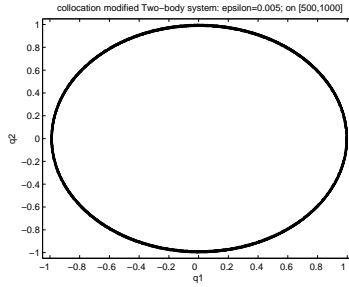


FIGURE 13. Phase plot of  $q_1$  and  $q_2$  when  $\epsilon = 0.005$  by collocation method on  $[500,1000]$ ,  $N = 20$ ;

	time(secs)	Error in Energy	Error in Angular Momentum
Colloc,N=20,[0, 10 <sup>4</sup> ]	4950	$2.15614193 \times 10^{-11}$	$2.09121608 \times 10^{-11}$
Colloc,N=20,[0,1000]	52	$2.15372164 \times 10^{-12}$	$2.08877359 \times 10^{-12}$
Symp 1,h=0.001,[0,75]	53	$6.05561933 \times 10^{-8}$	$5.85881273 \times 10^{-8}$
Symp 1,h=0.001,[0,80]	72	$6.48879968 \times 10^{-8}$	$6.18349377 \times 10^{-8}$

TABLE 7. Comparison of CPU times between the two methods.

	time(secs)	Error in Energy	Error in Ang. Momentum
Colloc, N=20 on [0,100]	3	$4.28660520 \times 10^{-7}$	$1.3618605 \times 10^{-7}$
Symp 1,h=0.001,[0,40]	75	$3.02104066 \times 10^{-7}$	$1.06633042 \times 10^{-6}$
Symp 1,h=0.001,[0,50]	166	$3.02104066 \times 10^{-7}$	$1.06633042 \times 10^{-7}$

TABLE 8. Comparison of CPU times between the two methods with the same order of errors when  $\epsilon = 0$ .

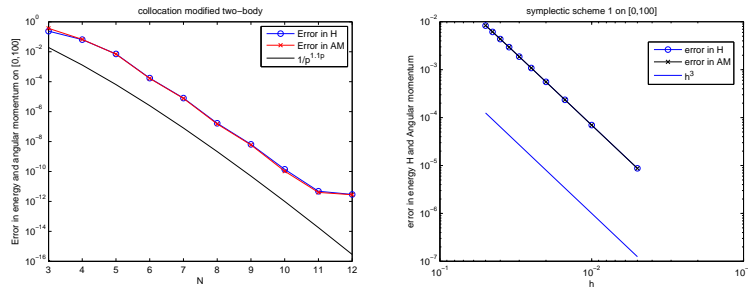


FIGURE 14. (a) Error in  $H$  and the angular momentum with  $(\frac{1}{N})^{(1.1N)}$  versus  $N = 3, 4, \dots, 12$  by the spectral collocation on  $[0, 100]$ ; (b) Error in  $H$  and the angular momentum versus  $h=0.005, 0.01, 0.015, \dots, 0.05$ , on  $[0, 100]$  by symplectic 1.

Consider the Hamiltonian of the Earth-Moon-Satellite system given by

$$H(p_x, p_y, x, y) = \frac{p_x^2 + p_y^2}{2} + (yp_x - xp_y) - \left( \frac{(1 - \mu)}{r_1} + \frac{\mu}{r_2} \right),$$

where  $r_1^2 = (x + \mu)^2 + y^2$ ,  $r_2^2 = (x + \mu - 1)^2 + y^2$ .

This model describes the motion of the satellite around the Earth and Moon. The Earth and Moon are located on the x-axis where their center of mass is placed at the origin. The coordinate of the satellite is  $(x, y)$ . It rotates in the orbit around the Earth and Moon at the rate one moon month so the Earth and Moon are always on the x-axis. The mass of the Moon is  $\mu = 0.01215$  (the length unit is 384400 km).

The corresponding system is given by

$$\begin{aligned} p'_x(t) &= p_y - \frac{(1-\mu)}{r_1^3}(x+\mu) - \frac{\mu}{r_2^3}(x+\mu-1) \\ p'_y(t) &= -p_x - \frac{(1-\mu)}{r_1^3}y - \frac{\mu}{r_2^3}y \\ x'(t) &= p_x + y \\ y'(t) &= p_y - x \end{aligned}$$

We compare the spectral collocation with a second order symplectic method under a transformation  $q_1 = \frac{1}{2}(x+y)$ ,  $q_2 = \frac{1}{2}(x-y)$ ,  $p_1 = p_x + p_y$ ,  $p_2 = p_x - p_y$ . The initial conditions for Figure 15 are  $p_1(0) = 1.259185$ ,  $p_2(0) = -1.259185$ ,  $q_1(0) = -0.25$ ,  $q_2(0) = -0.25$  where we can see an orbit (the coordinate plot for this case is a circle (not shown)) and  $p_1(0) = -0.16$ ,  $p_2(0) = -0.7$ ,  $q_1(0) = 1.3$ ,  $q_2(0) = -0.31$  for Figure 16 to observe the orbit of the satellite. Solutions are plotted using the same frame sizes. In Figure 15, the orbit from a symplectic method is thicker than the collocation method especially at the left and right corner.

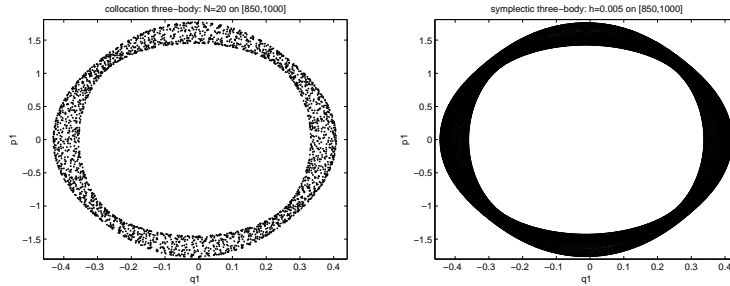


FIGURE 15. Phase plot  $p_1$  versus  $q_1$  of the orbit by (a) spectral collocation on [850, 1000]; (b) Symplectic 1  $h=0.005$  on [850, 1000].

Table 9 compares the error in energy  $H$  and the CPU times by using the first set of the initial conditions. We use  $h = 0.005$  for the symplectic method. At  $t = 300$ , the spectral collocation method uses much less time (5.4 second vs. 18 second) and yet, offers much better accuracy in energy ( $2 \times 10^{-7}$ ) than the symplectic method ( $9 \times 10^{-3}$ ).

The convergence rates of each method are plotted in Figure 17. The rate for spectral collocation is of order  $(\frac{1}{N})^{(0.33N)}$  and for Symplectic 1 is of order three.

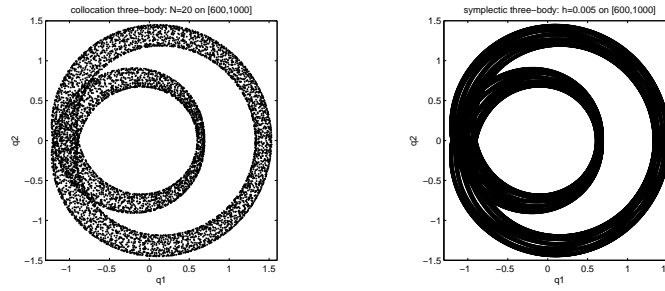


FIGURE 16. Phase plot of the coordinate of the satellite,  $q_2$  versus  $q_1$  by (a) spectral collocation on  $[600, 1000]$ ; (b) Symplectic 1  $h=0.005$  on  $[600, 1000]$ .

	time(secs)	Error in Energy
Collocation, $N=20$ on $[0, 300]$	5.4	$1.9090052472 \times 10^{-4}$
Symplectic 1 on $[0, 300]$	18	$9.3757448742 \times 10^{-3}$
Symplectic 1 on $[0, 150]$	4.6	$4.8046166186 \times 10^{-3}$

TABLE 9. Comparison of CPU times between the two methods.

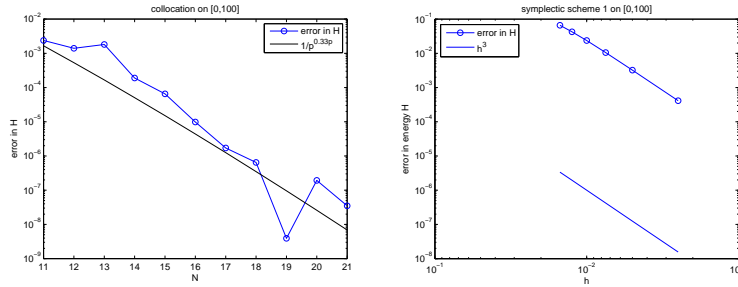


FIGURE 17. (a) Error in  $H$  with  $(\frac{1}{N})^{(0.33N)}$  versus  $N = 11, 12, \dots, 21$  by spectral collocation on  $[0, 100]$ ; (b) Error in  $H$  versus  $h = 0.0025, 0.005, \dots, 0.015$  by Symplectic 1 on  $[0, 100]$ .

### 5. Conclusion remarks

We have compared numerically a spectral collocation method and several symplectic methods in solving Hamiltonian dynamical systems. Our numerical evidences have demonstrated that the spectral collocation method has several advantages.

- 1) It requires less CPU times in order to reach the same accuracy.
- 2) It preserves energy and symplectic structure better.
- 3) It predicts more accurate trajectories for long time.

In addition, the proposed collocation method is systematic and can be applied to any Hamiltonian system without changing the basic algorithm. On the other hand, one needs to design different symplectic methods for different problems. A

theoretical investigation for the stability, convergence, and symplectic preserving properties of the spectral collocation method is underway.

## References

- [1] V.I. Arnold, *Mathematical Methods of Classical Mechanics*, Springer, New York, 1978.
- [2] C. Bernardi and Y. Maday, Spectral Methods. In *Handbook of Numerical Analysis*, Vol. V, P.G. Ciarlet and J.-L. Lions eds., North-Holland (1997), 209-485.
- [3] J.P. Boyd, *Chebyshev and Fourier Spectral Methods*, 2nd edition, Dover, New York, 2001.
- [4] M.P. Calvo and J.M. Sanz-Serna, Instabilities and inaccuracies in the integration of highly oscillatory problems, *SIAM J. Sci. Comput.* (to appear).
- [5] C. Canuto, M.Y. Hussaini, A. Quarteroni, and T.A. Zang, *Spectral Methods in Fluid Dynamics*, Springer-Verlag, New York, 1988.
- [6] C. Canuto, M.Y. Hussaini, A. Quarteroni, and T.A. Zang, *Spectral Methods: Fundamentals in Single Domains*, Springer Series: Scientific Computation, Berlin, 2006.
- [7] D. Cohen, E. Hairer and C. Lubich, Numerical energy conservation for multi-frequency oscillatory differential equations, *BIT* 45 (2005) 287-305.
- [8] D. Cohen, E. Hairer, and C. Lubich, Conservation of energy, momentum and actions in numerical discretizations of nonlinear wave equations, *Numerische Mathematik* 110 (2008) 113-143.
- [9] E. Faou, E. Hairer and, T.-L. Pham, Energy conservation with non-symplectic methods: examples and counter-examples, *BIT* 44 (2004) 699-709.
- [10] K. Feng, On difference schemes and symplectic geometry. In: *Proceedings of the 1984 Beijing Symposium on Differential Geometry and Differential Equations* (K. Feng editor), pp.42-58, Science Press, Beijing, 1985.
- [11] K. Feng, Difference schemes for Hamiltonian formalism and symplectic geometry, *J. Comput. Maths.*, 4 (1986), 279-289.
- [12] K. Feng, How to compute properly Newton's equation of motion?. In: *Proceedings of 2nd Conf on Numerical Methods for Partial Differential Equations* (L.A. Ying, B.Y. Guo editors), Singapore, pp.15-22, World Scientific, 1992.
- [13] K. Feng, The Hamiltonian way for computing Hamiltonian dynamics. In: *Applied and Industrial Mathematics. Netherlands: Kluwer* (R. Spigler editor), pp.17-35, Kluwer Academic, 1991.
- [14] K. Feng, M.Z. Qin, *Symplectic Geometric Algorithms for Hamiltonian Systems*, Zhejiang Science and Technology Press, Hangzhou, 2003.
- [15] K. Feng, M.Z. Qin, The symplectic methods for the computation of Hamiltonian equations, *Lect. Notes in Math.*, 1297 (1987), 1-37.
- [16] K. Feng, D.L. Wang, Variations on a theme by Euler, *J. Comput. Maths.*, 12 (1998), 97-106.
- [17] K. Feng, H.M. Wu, M.Z. Qin, D.L. Wang, Construction of canonical difference schemes for Hamiltonian formalism via generating functions, *J. Comput. Maths.*, 7 (1989), 71-96.
- [18] B. Garia-Archilla, J.M. Sanz-Serna, and R.D. Skeel, Long-Time-Step Methods for Oscillatory Differential Equations, *SIAM J. Sci. Comput.* 20-3 (1999).
- [19] G. Zhong and J.E. Marsden, Lie-Poisson Hamilton-Jacobi theory and Lie-Poisson integrators, *Phys. Lett. A* 133-3 (1988), 134-139.
- [20] D. Gottlieb and T.A. Orszag, *Numerical Analysis of Spectral Methods: Theory and Applications*, SIAM, Philadelphia, 1977.
- [21] B.-Y. Guo, *Spectral Methods and their Applications*, World Scientific, Singapore (1998).
- [22] B.-Y. Guo and Z.-Q. Wang, Legendre-Gauss collocation methods for ordinary differential equations, *Adv. Comput. Math.* 30 (2009), 249-280.
- [23] E. Hairer, Long-time energy conservation of numerical integrators, *Foundations of Computational Mathematics*, Santander 2005, London Math. Soc. Lecture Notes Ser. 331, Cambridge University Press (2006), 162-180.
- [24] E. Hairer and C. Lubich, Symmetric multistep methods over long times, *Numer. Math.* 97 (2004), 699-723.
- [25] E. Hairer and C. Lubich, Spectral semi-discretisations of weakly nonlinear wave equations over long times, *Found. Comput. Math.* 8 (2008), 319-334.
- [26] E. Hairer, C. Lubich, and G. Wanner, *Geometric Numerical Integration: Structure-Preserving Algorithms for Ordinary Differential Equations*, Springer Series in Comput. Mathematics, vol. 31. Springer-Verlag, Berlin (2002).

- [27] G.E. Karniadakis and S.J. Sherwin, *Spectral/hp Element Methods for CFD*, Oxford University Press, New York, 1999.
- [28] W. Lu, H. Zhang and S. Wang, Application of Symplectic Algebraic Dynamics Algorithm to Circular Restricted Three-Body Problem, *Chin. Phys. Lett.* 25 (2008) 2342-2345.
- [29] J.E. Marsden, G. Misiulek, J.-P. Ortega, M. Perlmutter, and T.S. Ratiu, *Hamiltonian Reduction by Stages*, Lecture Notes in Mathematics, Springer Berlin, 2007.
- [30] J.E. Marsden and M. West, Discrete mechanics and variational integrators, in: *Acta Numerica* 2001, 357-514.
- [31] R. Peyret, *Spectral Methods for Incompressible Viscous Flow*, Springer, New York, 2002.
- [32] J.M. Sanz-Serna, Symplectic integrators for Hamiltonian problems: an overview, in: *Acta Numerica* 1992, 243-286.
- [33] J.M. Sanz-Serna and M.P. Calvo, *Numerical Hamiltonian Problems*, Chapman & Hall, 1994.
- [34] J. Shen and T. Tang, *Spectral and High-Order Methods with Applications*, Science Press, Beijing, 2006.
- [35] J. Shen and L.-L. Wang, Fourierization of the Legendre-Galerkin method and a new space-time spectral method, *Applied Numerical Mathematics*, 57 (2007), 710-720.
- [36] A.M. Stuart and A.R. Humphries, *Dynamical Systems and Numerical Analysis*, Cambridge University Press, 1996.
- [37] L.N. Trefethen, *Spectral Methods in Matlab*, SIAM, 2000.
- [38] H. Van de Vyver, A fourth-order symplectic exponentially fitted integrator, *Computer Phys. Comm.*, 174 (2006), 255-262.
- [39] T. Wu, C. Shen, G. Ju, N. Ju, Application of symplectic algorithm to QCT calculation:  $H + H_2$  system, *Science in China(Series B)*, 45 (2002), 15-20.
- [40] Z. Zhang, Superconvergence of Spectral collocation and p-version methods in one dimensional problems, *Math. Comp.*, 74 (2005), 1621-1636.
- [41] Z. Zhang, Superconvergence of a Chebyshev spectral collocation method, *Journal of Scientific Computing* 34 (2008) 237-246.

## Appendix

**Scheme 1:** Second order midpoint Euler Scheme [10].

This is an implicit method. Let  $z = (p_1, p_2, \dots, p_n, q_1, \dots, q_n)$ ,

$$J = \begin{pmatrix} 0 & I_n \\ -I_n & 0 \end{pmatrix} \text{ so } J^{-1} = \begin{pmatrix} 0 & -I_n \\ I_n & 0 \end{pmatrix} = -J, \quad H_z = [H_{p_1}, \dots, H_{p_n}, H_{q_1}, \dots, H_{q_n}]^T$$

$$\frac{1}{h}(z^{k+1} - z^k) = J^{-1}H_z\left(\frac{1}{2}z^{k+1} + \frac{1}{2}z^k\right).$$

Simply written as

$$\begin{aligned} p_i^{k+1} &= p_i^k - hH_{q_i}\left(\frac{1}{2}(p^{k+1} + p^k), \frac{1}{2}(q^{k+1} + q^k)\right) \\ q_i^{k+1} &= q_i^k + hH_{p_i}\left(\frac{1}{2}(p^{k+1} + p^k), \frac{1}{2}(q^{k+1} + q^k)\right), \quad i = 1, \dots, n. \end{aligned}$$

For a linear system, we can replace the right hand side as

$$\frac{1}{h}(z^{k+1} - z^k) = J^{-1}\left[\frac{1}{2}H_z(z^{k+1}) + \frac{1}{2}H_z(z^k)\right].$$

or

$$\begin{aligned} p_i^{k+1} &= p_i^k - h\frac{1}{2}[H_{q_i}(p^{k+1}, q^{k+1}) + H_{q_i}(p^k, q^k)] \\ q_i^{k+1} &= q_i^k + h\frac{1}{2}[H_{p_i}(p^{k+1}, q^{k+1}) + H_{p_i}(p^k, q^k)]. \end{aligned}$$

The equivalent scheme is symplectic for the linear system only. It is not symplectic for nonlinear system.

**Scheme 2:** Second order scheme [17].

$$\begin{aligned} p_i^{k+1} &= p_i^k - hH_{q_i}(p^{k+1}, q^k) - \frac{h^2}{2} \sum_{j=1}^n (H_{q_j} H_{p_j})_{q_i}(p^{k+1}, q^k) \\ q_i^{k+1} &= q_i^k + hH_{p_i}(p^{k+1}, q^k) + \frac{h^2}{2} \sum_{j=1}^n (H_{q_j} H_{p_j})_{p_i}(p^{k+1}, q^k), \quad i = 1, \dots, n. \end{aligned}$$

Note:  $\sum_{j=1}^n (H_{q_j} H_{p_j})_{q_i} (p^{k+1}, q^k) = \sum_{j=1}^n (H_{q_j} H_{p_j})_{q_i} (p_1^{k+1}, \dots, p_n^{k+1}, q_1^k, \dots, q_n^k)^T$ .  
 For  $n=1$ ,

$$\begin{aligned} p^{k+1} &= p^k - hH_q(p^{k+1}, q^k) - \frac{h^2}{2}(H_{q_q}H_p + H_{p_q}H_q)(p^{k+1}, q^k) \\ q^{k+1} &= q^k + hH_p(p^{k+1}, q^k) + \frac{h^2}{2}(H_{q_p}H_p + H_{p_p}H_q)(p^{k+1}, q^k). \end{aligned}$$

**Scheme 3:** Second order scheme for the three axis-symmetric Hamiltonian system [16].

$$\begin{aligned} P_1 &= p + \frac{\sqrt{3}}{4}h \sin\left(\frac{1}{2}p + \frac{\sqrt{3}}{2}q\right) \\ Q_1 &= q - \frac{1}{4}h \sin\left(\frac{1}{2}p + \frac{\sqrt{3}}{2}q\right) \\ P_2 &= P_1 - \frac{\sqrt{3}}{4}h \sin\left(\frac{1}{2}P_1 - \frac{\sqrt{3}}{2}Q_1\right) \\ Q_2 &= Q_1 - \frac{1}{4}h \sin\left(\frac{1}{2}P_1 - \frac{\sqrt{3}}{2}Q_1\right) \\ P_3 &= P_2 - \frac{\sqrt{3}}{4}h \sin\left(\frac{1}{2}P_2 - \frac{\sqrt{3}}{2}Q_2\right) \\ Q_3 &= Q_2 - h \sin(P_2) \\ Q_4 &= Q_3 - \frac{1}{4}h \sin\left(\frac{1}{2}P_3 - \frac{\sqrt{3}}{2}Q_3\right) \\ \hat{p} &= P_3 + \frac{\sqrt{3}}{4}h \sin\left(\frac{1}{2}P_3 + \frac{\sqrt{3}}{2}Q_4\right) \\ \hat{q} &= Q_4 - \frac{1}{4}h \sin\left(\frac{1}{2}P_3 + \frac{\sqrt{3}}{2}Q_4\right) \end{aligned}$$

**Scheme 4:** Second order scheme for the Henon-Heiles(HH) system [15].

$$\begin{aligned} p_1^{k+1} &= p_1^k - h(q_1^k + 2q_1^k q_2^k) \\ p_2^{k+1} &= p_2^k - h(q_2^k + (q_1^k)^2 - (q_2^k)^2) \\ q_1^{k+1} &= q_1^k + hp_1^{k+1} \\ q_2^{k+1} &= q_2^k + hp_2^{k+1} \end{aligned}$$

Department of Mathematics, Wayne State University, Detroit, MI 48202, USA  
*E-mail:* [nairat@math.wayne.edu](mailto:nairat@math.wayne.edu) and [zzhang@math.wayne.edu](mailto:zzhang@math.wayne.edu)